Two Functional States of the CD11b A-Domain: Correlations with Key Features of Two Mn^{2+}-complexed Crystal Structures

Rui Li, Philippe Rieu, Diana L. Griffith, David Scott, and M. Amin Arnaout

Leukocyte Biology and Inflammation Program, Renal Unit, Department of Medicine, Massachusetts General Hospital and Harvard Medical School, Charlestown, Massachusetts 02129

Abstract. In the presence of bound Mn^{2+}, the three-dimensional structure of the ligand-binding A-domain from the integrin CR3 (CD11b/CD18) is shown to exist in the "open" conformation previously described only for a crystalline Mg^{2+} complex. The open conformation is distinguished from the "closed" form by the solvent exposure of F302, a direct T209–Mn^{2+} bond, and the presence of a glutamate side chain in the MIDAS site. Approximately 10% of wild-type CD11b A-domain is present in an "active" state (binds to activation-dependent ligands, e.g., iC3b and the mAb 7E3). In the isolated domain and in the holoreceptor, the percentage of the active form can be quantitatively increased or abolished in F302W and T209A mutants, respectively. The iC3b-binding site is located on the MIDAS face and includes conformationally sensitive residues that undergo significant shifts in the open versus closed structures. We suggest that stabilization of the open structure is independent of the nature of the metal ligand and that the open conformation may represent the physiologically active form.

Key words: integrin activation • A-domain • crystal structure • complement iC3b • G proteins

The interaction of integrins with their ligands is an essential step in regulating many cellular functions (reviewed in Hynes, 1992). Integrin binding to various ligands is divalent cation dependent, and is tightly regulated by inside-out and outside-in signaling events. The mechanisms through which these signals modulate integrin–ligand interactions are not known. Biophysical, biochemical, and immunochemical studies have revealed that integrins exist in low and high affinity states (Du et al., 1993). Activation signals lead to conformational changes that extend to the receptor's extracellular ligand-binding regions (Diamond and Springer, 1993; Landis et al., 1993; Bilsland et al., 1994; Kamata and Takada, 1994; Randi and Hogg, 1994; Zhou et al., 1994). It has also been proposed that rapid oscillations between the low and high affinity states of integrins contribute to the adhesion–deadhesion cycles during cell migration and cytolysis (Dransfield et al., 1992).

Recent studies in several integrins have identified two major ligand-binding sites. One is located within an A-type domain (A- or I-domain) present in the α subunits of seven integrins (Diamond et al., 1993; Michishita et al., 1993; Landis et al., 1994; Randi and Hogg, 1994; Zhou et al., 1994; Tuckwell et al., 1995; Xie et al., 1995). A second region is located in a highly conserved segment of all the integrin β subunits (D'Souza et al., 1988; Smith and Cheresh, 1988; Andrew et al., 1994; Bajt and Loftus, 1994; D'Souza et al., 1994; Kamata et al., 1995*a*). Secondary structure, hydropathy, and protein threading algorithm predict that this segment also adopts an A-type fold (Lee et al., 1995*b*; Arnaout, M.A., unpublished observations), suggesting that structure–function analysis of the A-domain is likely to shed light on the structural basis of affinity switching in all integrins.

The recombinant CD11b A-domain (r11bA) from the β2 integrin CR3 (CD11b/CD18, αMβ2) binds directly to several ligands in a divalent cation–dependent manner (Michishita et al., 1993; Lee et al., 1995*b*). Some of these ligands (e.g., iC3b, fibrinogen, CD54 [ICAM-1], and the ligand-mimetic mAb 7E3) can only interact with the holoreceptor in its active state. Others such as neutrophil inhibitory factor (NIF)[1] bind to CR3 regardless of its activa-

Address correspondence to M. Amin Arnaout, M.D., Renal Unit, Massachusetts General Hospital and Harvard Medical School, 149 13th Street, 8th Floor, Charlestown, MA 02129. Tel.: (617) 726-5663. Fax: (617) 726-5669. E-mail: arnaout@receptor.mgh.harvard.edu

1. *Abbreviations used in this paper:* MFI, mean fluorescence intensity; MIDAS, metal ion–dependent adhesion site; NIF, neutrophil inhibitory factor; WT, wild-type.

tion status (Michishita et al., 1993; Rieu et al., 1994; Ueda et al., 1994; Zhou et al., 1994; Lee et al., 1995*b*; Xie et al., 1995). The ability of both activation-dependent and -independent ligands to bind to r11bA suggests that the r11bA either becomes active when removed from the holoreceptor or exists in different affinity states. The crystal structures of several integrin A-domains have been published. The structures invariably include a dinucleotide-binding fold (similar to that of small G proteins where the fold was first described), a buried β sheet surrounded by amphipathic helices (seven in CD11b A-domain), and a solvent-exposed metal ion located in a crevice at the COOH-terminal end of the β sheet. The metal ion is coordinated by a group of conserved amino acids forming the metal ion–dependent adhesion site (MIDAS). The first published structure of r11bA complexed to Mg^{2+} (Lee et al., 1995*b*) ("open" form) showed significant differences from a second "closed" conformation of r11bA complexed to Mn^{2+} (Lee et al., 1995*a*; Baldwin et al., 1998) and from all CD11a crystal structures (Qu and Leahy, 1995): in the open form, a glutamate from a neighboring molecule provides the sixth metal coordination site. In addition, two phenylalanines (F275 and F302) are solvent exposed due to conformational changes that involve several loops. Based on mechanistic similarities with the "active" and "inactive" structures of the signaling proteins ras and Gα, we suggested that this open form is active while the closed conformation is inactive (Lee et al., 1995*a*). Because the open and closed states of r11bA formed in the presence of different metal ions (Mg^{2+} and Mn^{2+}, respectively) and because of the uniformly activating effect of Mn^{2+} on integrins, a counterargument was made that the Mn^{2+}-complexed form represents the active species (Qu and Leahy, 1995). More recently, it was argued based on theoretical considerations that the open form is a structural artifact that arises secondary to a truncated COOH terminus (Baldwin et al., 1998).

In this communication, we demonstrate that r11bA crystallized in the presence of Mn^{2+} can also assume the open conformation, indicating that generation of this structure is independent of the nature of the metal ion. The functional relevance of the structural changes observed between the open and the closed conformations (changes in MIDAS topology, solvent exposure of F302 and F275, and coordination of the metal ion to T209) was probed through mapping of the iC3b-binding site and by mutational analysis of certain conformationally sensitive residues. The binding site in CR3 for iC3b incorporates conformationally sensitive residues that move up to 3.5 Å in the two structures (relative to the bound manganese metal ion). F302W and F275R substitutions that introduce bulky or charged residues at these two positions, respectively, increased r11bA (and holoreceptor) binding to activation-dependent ligands. On the other hand, a T209A substitution, intended to abolish the direct T209–metal coordination found in the open form, resulted in a complete loss of r11bA (and holoreceptor) binding to activation-dependent ligands. However, none of these mutants affected the interaction of r11bA or the holoreceptor with the activation-independent ligand NIF. Analysis of the interaction of wild-type (WT) r11bA with iC3b using surface plasmon resonance identified active and inactive populations of the A-domain, with the latter predominating. The proportion of the active form increased by 2.5-fold in the F302W domain compared with WT and disappeared by the T209A substitution. We suggest that the active and inactive states may correspond to the open and closed crystal structures, respectively.

Materials and Methods

Reagents and Antibodies

Restriction and modification enzymes were purchased from New England Biolabs Inc. (Beverly, MA), Boehringer Mannheim (Mannheim, Germany), or GIBCO BRL (Gaithersburg, MD). The anti-CD11b mAbs OKM10, 44, 903, 904, 7E3, and the anti-CD18 mAb TS1/18 have been described previously (Arnaout et al., 1983; Coller, 1985; Dana et al., 1986; Wright et al., 1987). Purified fibrinogen was a kind gift from Dr. Jari Ylanne (University of Helsinki, Helsinki, Finland). mAb 7E3 and FITC-conjugated 7E3 were gifts from Dr. Barry S. Coller (Mount Sinai Medical Center, New York).

Site-directed Mutagenesis

This was carried out in pcDNA3 or πH3M expression vectors as described (Kunkel et al., 1987; Deng and Nicoloff, 1992). Some of the primers used have been published elsewhere (Rieu et al., 1996). The following additional mutagenic primers were used, each followed by the introduced unique restriction site: F302R reverse, CTGAATGGTCTTAAGAGCCTCTCTGTTATTCACCTG (AflII); F302W forward, CGTGTTCCAGGTGAATAACTGGGAAGCTTTGAAGACCATTCAGAACC (HindIII); F302Y reverse, CTGAATGGTCTTAAGAGCCTCGTAGTTATTCACCTG (AflII); F275R reverse, TTGGCGGGATTTCTCGGACCGTCTGGCATCTCCCACCCC (RsrII); T209A forward, CTGCTTGGGCGAGCTCACACGGCCACG (SacI); G247A forward, CGGATGGAGAAAAGTTTGCGGATCCCTTGGGATATGA (BamHI); and P249A forward, GGAGAAAAGTTTGGCGATGCCTTGGGATATGAGGACGTCATCCCT (AatII). Each mutation was confirmed by the presence of the introduced restriction site and by direct DNA sequencing (Sanger et al., 1977). The recombinant DNA work used standard protocols (Maniatis et al., 1989).

Protein Purification and Characterization

Recombinant WT r11bA and its mutants F302W, T209A, and D140GS/AGA were expressed as GST fusion proteins in *Escherichia coli*, as described elsewhere (Michishita et al., 1993; Ueda et al., 1994). cDNA sequencing of the 3′ end of the WT and mutant r11bA constructs predicts a protein that terminates with A318 of CD11b plus the vector sequence GNSS. The fusion proteins were purified by affinity chromatography on glutathione-coupled beads, and cleaved with thrombin to release the recombinant A-domains. WT and mutant r11bA were further purified by ion exchange chromatography on a Mono S HR5/5 column using the FPLC system (both from Pharmacia, Piscataway, NJ). Analysis of the purified proteins on 12% SDS-PAGE revealed a single band of the expected size after staining with Coomassie blue (data not shown).

The purified thrombin-cleaved WT r11bA was digested overnight with immobilized TPCK-trypsin (Pierce, Rockford, IL) as described (Lee et al., 1995*b*), and then repurified by gel filtration on a Superdex-75 column. The NH_2 terminus of the trypsin-treated r11bA begins with G127, as determined by protein sequencing. The COOH termini of both thrombin- and trypsin-treated preparations were sequenced using the Mayo Protein Core Facility and were found to be identical. Both proteins end with A318 of the native domain followed by the vector-derived sequences GD (instead of the predicted N), with the two COOH-terminal serines detected in lower quantities (data not shown).

The thrombin- and trypsin-treated preparations were also analyzed by LC-MS using MassLynx software. The measured mass of the thrombin-cleaved protein is 24,235.8 (calculated mass using monoisotopic masses based on the predicted 212–amino acid peptide is 24,143.5; *measured − calculated mass* [Δ] = 92.3; expected measured error of +0.02%). The measured mass of the limited trypsin-cleavage product (beginning with G127 and ending with GNSS) is 22,383.7 (calculated 22,293.6, Δ = 90.1). LC-MS analysis of the tryptic sequence fragments resulting from an ex-

haustive digest of the thrombin-cleaved A-domain allowed an assignment of all of the sequence up to R313. By difference, the mass of the COOH-terminal sequence (E314KIFAGNSS) must be 1025.7 (calculated 952.2, Δ = 73.5), suggesting that a modification in the COOH-terminal sequence (most likely in the vector sequence) is responsible for the larger measured mass of the domain.

Crystallization

The trypsin-treated r11bA was desalted on a Bio-Gel P-6DG column (BIO-RAD, Richmond, CA) and concentrated to 16 mg/ml for crystallization using a centricon unit with a 10 K molecular mass cutoff (Amicon Inc., Beverly, MA). Crystals were grown using the hanging drop vapor diffusion method by mixing equal volumes (5 μl) of protein and reservoir solution (23% polyethylene glycol 8 K, 0.05 M Tris, pH 8.8, 100 mM $MnCl_2$), at room temperature (modified from Lee et al., 1995*b*). Crystals started to form within a week, grew to a typical size of 0.3 mm × 0.05 mm × 0.04 mm in 3–4 wk, and belonged to the tetragonal space group $P4_3$ (Table I). These crystals are isomorphous with the Mg^{2+}-containing crystals (Lee et al., 1995*b*).

Data Collection and Structure Determination

A single crystal was used to collect a 2.7Å resolution data set, at 100 K, on beamline X25 of the National Synchrotron Light Source at the Brookhaven National Laboratory using a MarResearch imaging plate detector. Data were processed with DENZO and SCALEPACK (Otwinowski, 1991) to an R_{sym} of 12.2%. The starting model was the refined 1.8 Å Mg^{2+} structure (pdb accession code lido) (Lee et al., 1995*b*) comprising residues D132 to K315, with the metal and water molecules removed. The structure was refined using the computer program PROFFT (Finzel, 1987) to a final R factor of 19.8% (1.5 sigma cutoff). The final model comprises all nonhydrogen atoms of residues D132 to K315, 25 water molecules, and one manganese metal ion. Water molecules were placed and maintained based on suitable peaks in difference maps, reasonable hydrogen bond arrangements, and refined temperature factors of <35. Five protein residues have energetically unfavorable phi-psi angles as demonstrated by a Ramachandran plot (Gln163, Thr169, Ser177, Phe184, and Leu206), and include one of the residues also noted in the 1.8Å structure (Ser177). Examination of hydrogen bonding patterns and local interactions suggest plausible explanations for the unusual geometry of four of the five residues.

COS Cell Transfections

COS M7 simian fibroblastoid cells at 60–70% confluence were transfected with supercoiled cDNAs encoding WT and mutant CD11b and CD18 as described (Michishita et al., 1993). Transfected COS cells were grown for 24 h in Iscove's modified Dulbecco's medium (BioWhittaker, Inc., Walkersville, MD) supplemented with 10% FBS, 2 mM glutamine, 50 IU/ml penicillin and streptomycin at 37°C. Cells were then washed, detached with 0.1% trypsin-EDTA, and seeded in replicates for 24 h onto 24- or 48-well plates (Costar Corp., Cambridge, MA) or 100-mm petri dishes. Confluent monolayers in 24- or 48-well plates were then used for cell-surface antigen quantification and ligand-binding studies and those on petri dishes for immunoprecipitation studies.

Table I. Data Collection and Summary of Refinement Results

Space group: $P4_3$		
Unit cell: a = b = 45.15, c = 95.60		
Number of unique reflections = 4,305		
Percent completion = 81.7% (0 sigma)/67.8 (2 sigma)		
Average I/error = 6.8		
R-sym* = 12.2		
Resolution limits = 10.0–2.7 Å		
Refinement program = PROFFT		
R factor = 19.8 (1.5 sigma cutoff)		
Protein residues = D132–K315		
Number of water molecules = 25		
Number of metal (manganese) ions = 1		
Root mean square deviations from ideal values‡		
Bond lengths:	0.008 Å	sigma 0.030
Bond angle distances:	0.015 Å	sigma 0.040
Planarity:	0.013 Å	sigma 0.050

*Sum (Abs(I − <I>))/Sum (I).

‡Sigma values are the inverse square root of the restraint weight used during refinement. The coordinates will be deposited in the protein data bank.

Heterodimer Formation

This was assessed as described previously (Michishita et al., 1993). Confluent monolayers of transfected COS cells from 100-mm petri dishes were washed in PBS containing 5 mM EDTA, and each plate was solubilized in 0.5 ml of PBS containing 1% Triton X-100, 2 mM PMSF, 2 mg/ml leupeptin, and 2 mg/ml pepstatin A (Sigma Chemical Co., St. Louis, MO). The detergent-soluble fraction was harvested after centrifugation and immunoprecipitated using the anti-CD18 mAb TS1/18. Washed immunoprecipitates were separated by SDS-PAGE under reducing conditions (Laemmli, 1970) and electroblotted onto Immobilon-P membranes (Millipore Corp., Bedford, MA). After blocking with 10% nonfat milk in PBS, the membrane was incubated for 1 h with the anti-CD11b mAb 44 (Arnaout et al., 1983). Detection of proteins was performed using the enhanced chemiluminescence kit from Amersham Corp. (Buckinghamshire, UK).

Generation of CHO Cell Lines Expressing WT and Mutant CR3

The CHO-K1 cell line was maintained in Ham's F12 nutrient mixture (GIBCO BRL) supplemented with 10% FBS, 100 U/ml penicillin, and 100 μg/ml streptomycin. Transfection of CHO-K1 cells with WT or F302W CD11b and CD18 cDNA, in pcDNA3/Neo and πH3M plasmids, respectively, was performed using the calcium phosphate precipitation method as described previously (Golenbock et al., 1993). After 48 h, the medium was replaced with fresh medium containing 1 mg/ml of G418. The G418-resistant cell population was analyzed for CR3 expression with a FACScan® flow cytometer (Becton Dickinson, Mountain View, CA), and the CD11b and CD18 double-positive cells were enriched by cell sorting. The CHO cells expressing WT and F302W CR3 were then cloned by limiting dilution. CHO cells transfected with pcDNA/Neo alone were made and used as a negative control.

Preparation of Complement iC3b-coated Erythrocytes and Purification of iC3b

Sheep erythrocytes coated with complement iC3b were prepared as described (Michishita et al., 1993). EiC3b (1.5×10^8 cells/ml) were labeled with 5-(and-6)-carboxy fluorescein (Molecular Probes, Eugene, OR) (Ueda et al., 1994), washed, and resuspended to the original concentration for use in the binding studies. In some experiments, EiC3b cells were surface labeled with biotin by incubating the cells with 0.5 mg/ml sulfo-NHS-biotin (Pierce) for 30 min at 4°C.

iC3b was purified from fresh human serum by affinity chromatography as described (Ross et al., 1987; Cai and Wright, 1995). In brief, 50 ml human serum was treated with 20 mM iodoacetamide (Sigma) to block all free sulfhydryl groups. After extensive dialysis, the serum was incubated with 2–3 g of activated thiol-Sepharose 4B (Sigma) for 2 h at 37°C. The Sepharose activates the complement cascade, and the C3 is captured by thiol-Sepharose through its newly generated free sulfhydryl group. iC3b was eluted with 10 mM L-cysteine and further purified by ion exchange chromatography on a Mono Q HR5/5 column using FPLC system (both from Pharmacia). The purity of iC3b was examined on 8% SDS-PAGE.

mAb and Ligand Binding to WT or Mutant CR3-transfected COS and CHO Cells

Binding of mAbs, biotinylated NIF, or EiC3b to COS cells was assessed simultaneously as described (Michishita et al., 1993; Rieu et al., 1996). In brief, triplicate wells (from a 48-well plate) containing confluent-transfected COS cells were incubated with mAbs OKM10, 903, or TS1/18 (each at 2 μg/ml), or biotinylated NIF (at 400 ng/ml) in Tris-NaCl buffer, pH 7.4, containing 1 mM $MgCl_2$, 1 mM $CaCl_2$, 1% BSA (TMB buffer), and 0.02% sodium azide for 1 h at 4°C. Cells were then washed and incubated with ^{125}I-labeled goat anti–mouse immunoglobulin (New England Nuclear, Boston, MA) (for mAbs) or with ^{125}I-coupled avidin (Amersham, Arlington Heights, IL) (for NIF) under similar conditions. After washing, cells

were solubilized with 1% SDS, 0.2 N NaOH and the extracts were counted. Specific binding was obtained by subtracting the background binding to mock-transfected COS cells (usually <5% of total binding). The binding data from three independent experiments were pooled and expressed as histograms representing mean ± SEM, before the mutants were decoded. Binding of mAbs and NIF to COS cells was normalized for the percentage of binding obtained with WT as follows:% *binding* = (*mutant binding*/*WT binding*) × 100.

EiC3b binding was assessed by adding 40 μl of fluoresceinated EiC3b in TMB buffer to triplicate confluent wells (from a 24-well plate) in a total volume of 500 μl followed by a brief 15-s spin at 800 rpm/min. After a 5-min incubation at 37°C and two washes, the cells were solubilized with 1% SDS, 0.2 N NaOH and the fluorescence was quantified (excitatory wavelength, 490 nm; emission wavelength, 510 nm) using a SLM 8000 fluorometer (SLM Instruments, Urbana, IL) (Michishita et al., 1993). Specific binding was obtained by subtracting background binding to mock-transfected COS cells. Binding was normalized to the percentage of binding obtained with WT.

Purified iC3b and fibrinogen were diluted to 50 μg/ml and 50 μl of each diluted protein was placed in triplicates at the well center of 24-well non-tissue culture plates (Becton Dickinson). After incubating overnight at 4°C, the plates were washed and blocked with BSA. WT- or F302W-expressing CHO cells (10^6 in 400 μl of TMB buffer) were added to each well and incubated for 30 min at 37°C. After three washes, bound cells were quantified by detecting the cellular acid phosphatase level. Binding to Neo-transfected CHO cells was subtracted. Binding was normalized to the percentage of binding obtained with WT.

Flow Cytometry

WT-, F302W-, or Neo-transfected CHO cells were washed and resuspended in Ham's F12 nutrient mixture containing 2 mM $MnCl_2$ and 0.5% BSA to 6×10^6/ml. To a 50-μl cell suspension, FITC-conjugated mAbs 7E3, 44 (Sigma), or mouse IgG1 (Sigma) were added to a final concentration of 20 μg/ml, and incubated for 20 min at room temperature. The cells were washed, pelleted, resuspended in PBS containing 1% formaldehyde, and then analyzed immediately on a Becton Dickinson FACScan® flow cytometer. The fraction of CR3 recognized by 7E3 (high affinity CR3) was expressed as a ratio of the mean fluorescence intensity (MFI) generated by 7E3 to that generated by mAb 44 (which recognizes the whole population of expressed CR3) as follows: *high affinity CR3* (%) = (*MFI of 7E3*)/(*MFI of 44*) × 100.

mAb and Ligand Binding to Purified WT and Mutant r11bA

This was carried out on three different WT and F302W r11bA preparations as described (Ueda et al., 1994) with the following modifications. 50 μl of PBS, pH 7.4, containing 2 μg of WT or mutant r11bA was placed in triplicates in 96-well plates overnight at 4°C. Wells were washed, blocked with BSA, and then used in mAb or ligand-binding assays. Reactivity of r11bA with the anti-CD11b mAbs 44, 904, and 7E3 was assessed by incubating r11bA-containing wells with each mAb (10 μg/ml) for 1 h at room temperature, followed by a washing step, and a second incubation with alkaline phosphatase–coupled secondary antibody (Sigma) for an additional hour. Color reaction was then developed by adding 1 mg/ml *p*-nitrophenyl-phosphate, and quantified using a plate reader.

Binding of biotinylated EiC3b to immobilized WT or mutant r11bA was carried out by incubating 3×10^6 EiC3b cells in 50 μl veronal buffered saline, pH 7.4, containing 1 mM $MgCl_2$, 1 mM $CaCl_2$, and 0.1% gelatin, for 15 min at 37°C. After gentle washing, bound EiC3b were fixed with 1% glutaraldehyde, blocked with BSA, and treated with streptavidin–alkaline phosphatase conjugate and *p*-nitrophenyl-phosphate. Bound EiC3b was quantified by measuring the absorbance at 405 nm. Binding of biotinylated NIF to immobilized WT and mutant r11bA was carried out as described (Rieu et al., 1994). Background binding (binding to metal-defective mutant D140GS/AGA) was subtracted.

BIAcore™ Analysis

The apparent equilibrium constants for binding of three different preparations of WT and F302W r11bA to the complement fragment iC3b were measured using surface plasmon resonance on a BIAcore™ (BIAcore AB, Uppsala, Sweden). The Biosensor device was used in accordance with the manufacturer's instructions. In brief, iC3b was covalently coupled via primary amine groups to the dextran matrix of a CM5 sensor chip (BIAcore AB). BSA immobilized in the same way was used as a control surface. The WT and F302W A-domain proteins were flowed over the chip at 5 μl/min. TBS (20 mM Tris-HCl, pH 8.0, 150 mM NaCl) with 2 mM $MgCl_2$ and 0.005% P20 (BIAcore AB) was used as running buffer throughout. 1 M NaCl in 20 mM Tris-HCl, pH 8.0, was used to remove the bound proteins and to regenerate the surface for further binding experiments. The binding was measured as a function of time. The binding data (after subtracting background binding to BSA-coated chip) were analyzed using Scatchard plots as described (Dall'Acqua et al., 1996). For quantitatively determining the active proportion of the A-domain proteins, iC3b (an activation-dependent ligand) and mAb 904 (an activation- and metal-independent ligand) were each immobilized on a CM5 sensor chip. The WT and F302W A-domain proteins were flowed over the chip at 2 μl/min. The initial binding rates (obtained from linear regression of binding data over a 10–15-s period from the initial binding phase) under conditions of mass transfer limitation are proportional to the active protein concentration and independent of receptor-ligand affinity (Karlsson et al., 1993). Two different amounts of ligand (6,300 and 8,000 RU for iC3b; 4,200 and 6,200 RU for 904) were first used to examine the mass transfer limiting conditions. 100 mM HCl was used to regenerate the mAb 904 surface. The higher ligand densities of iC3b and 904 were used to determine the active proportion of the A-domain proteins.

Results and Discussion

Crystal Structure of the CD11b A-Domain in Complex with Mn^{2+}

The structure of r11bA crystallized in the presence of Mn^{2+} is nearly identical to that of the Mg^{2+} form (Lee et al., 1995*b*). The bound manganese ion is located in a shallow crevice at the top of the internal β sheet where it is coordinated by S142, S144, T209, and two water molecules. The sixth Mn^{2+} coordination site is provided by the side chain of E314 from a neighboring A-domain within the crystal lattice (Fig. 1 *A*). These structures are referred to as adopting the open conformation since F275 and F302 are solvent exposed (Fig. 1 *C*). The closed conformation (burial of F302, F275, or their equivalents into the hydrophobic core of the protein, a break in the T209 [or equivalent threonine]–metal bond; Fig. 1, *B* and *D*) and a corresponding change in surface charge and topology of MIDAS (Lee et al., 1995*a,b*; Qu and Leahy, 1995; Qu and Leahy, 1996; Emsley et al., 1997; Baldwin et al., 1998) are found in all remaining integrin A-domain structures determined to date. This includes the Mn^{2+} and no-metal forms of CD11bA, Mn^{2+} and Mg^{2+} forms of CD11aA, and a Mg^{2+}-complexed form of CD49bA. Taken together, these findings suggest that the integrin A-domain exists primarily in two conformations, the formation of which is unaffected by the nature of the metal ion in the active site or the experimental conditions of protein purification and crystal growth.

Mapping of the Binding Site for the Activation-dependent Ligand iC3b

We introduced single or double amino acid substitutions in residues scattered in all 11 loops and adjacent helices of the r11bA structure with the exception of the largely hydrophobic βC-α2 loop (H^{183}FT) and the α2-α3 loop (N^{192}PNP) (where a P195A substitution had detrimental effects on metal ion coordination; Michishita et al., 1993). All of the targeted residues had solvent-exposed side chains (relative total side chain accessibility values ranged from ~25 to 100%), and were replaced either with resi-

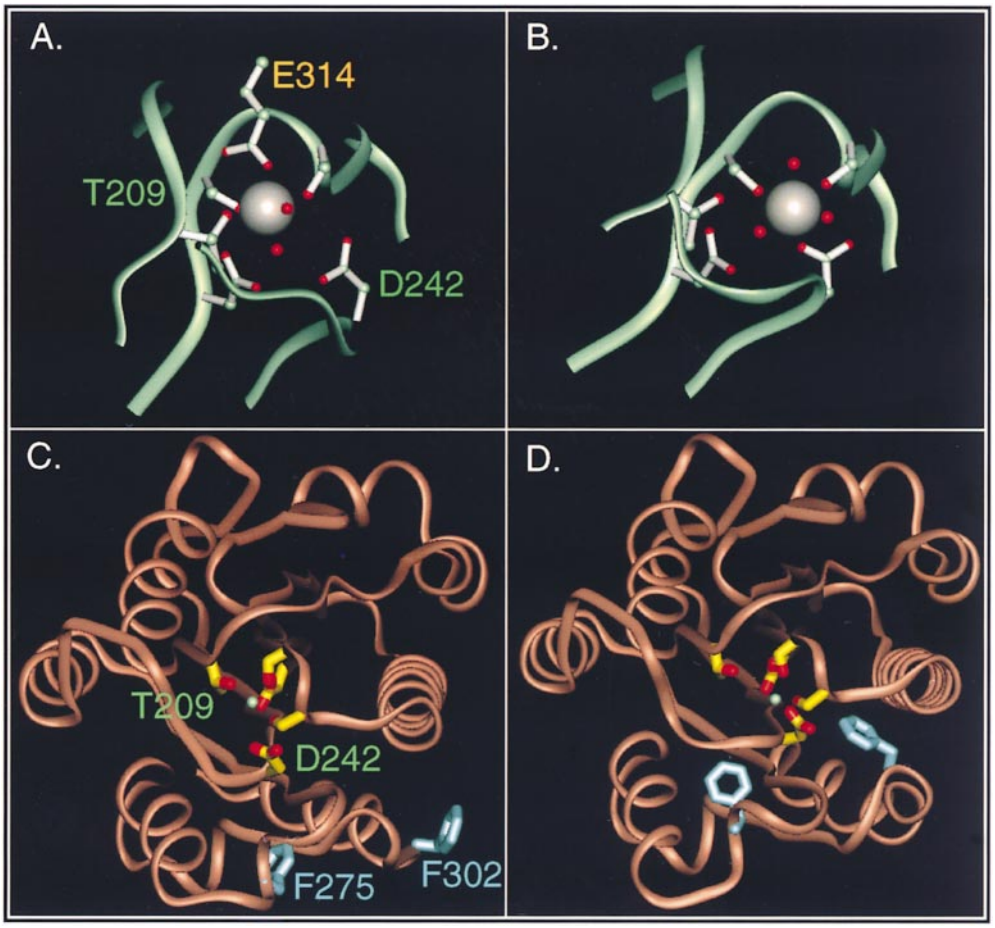

Figure 1. The Mn^{2+} structure of r11bA. *A* and *B* show a close-up of the MIDAS motif in the open (this report) and closed (Lee et al., 1995*a*) conformations, respectively. The Mn^{2+} metal ion in both forms is displayed in gray, oxygen atoms and water molecules are in red, and the protein backbone is shown schematically as a light green ribbon. *C* and *D* show a top view of r11bA structure (ribbon backbone) with the major changes in the open (*C*) (this report) and closed (*D*) Mn^{2+}-complexed conformations. The solvent-exposed Mn^{2+} is shown (*light green ball*) surrounded by the largely buried metal coordinating residues D140, S142, S144, T209, and D242 (side chains are outlined in yellow and red). F302 and F275 are shown in light blue. The figure was built using QUANTA (Molecular Simulations Inc., Mountain View, CA). See the text for details.

dues from CD11a (which does not bind to iC3b or NIF), with residues having the opposite charge, or with alanines. The WT and mutant receptors expressed in COS cells were then probed with mAbs or ligands as described (Michishita et al., 1993; Rieu et al., 1996). None of the mutations affected the normal expression of the receptors as judged by binding of the anti-CD11b mAbs OKM10 (Fig. 2 *A*), 903, and the anti-CD18 mAb TS1/18 (Rieu et al., 1996; and data not shown). Binding of G143M, D149K, E178E/AA, T203Q/KH, R208L, F246K, and E278K/AA receptors to iC3b was either absent or significantly reduced (Fig. 2 *B*), whereas that of E244K and D273K was significantly increased. Gain-of-function mutations are not unusual in contact regions of protein–protein complexes (Clackson and Wells, 1995). A smaller but still significant increase in binding of K166S/AA was also observed. None of the remaining eight mutations (involving 11 amino acids) affected iC3b binding significantly. The loss of iC3b binding to some mutants was not caused by defective formation of the heterodimer (Fig. 2 *B*, *inset*; Rieu et al., 1996) or an inability of the domain to bind metal: Mn^{54} bound directly to G143M, D149K, E178E/AA, and R208L r11bA mutants, and the metal-dependent interaction of biotinylated NIF with the remaining mutants T203Q/KH, E244K, F246K, D273K, and E278K/AA was normal (Rieu et al., 1996). With the exception of E278K and T203 (PQ and K, respectively, in mouse), the residues involved in iC3b binding were either identical (G143, D149, E179, Q204, R208, E244, and F246) or conserved (E178 and D273) in mouse CR3 (Pytela, 1988). This may explain the ability of mouse and human CR3 to bind to human and mouse iC3b, respectively. The relative affinity of these cross-species interactions has not been determined.

Previous studies have examined the structural basis of CR3 binding to iC3b. One study focused on residues in the βD-α5 loop (F246-Y252) adjacent to D242 (McGuire and Bajt, 1995), since these residues are absent in the non–iC3b-binding CD11a A-domain (Rieu et al., 1996), and peptides spanning this loop or immediately preceding it affect iC3b binding (Ueda et al., 1994). Deletion of the βD-α5 loop in human CR3 or a D248A substitution abolished receptor binding to iC3b (McGuire and Bajt, 1995). The βD-α5 loop was among those targeted in our mapping study, and replacement of one of its residues F246 with lysine (F246K) abolished iC3b binding, whereas G247A and P249A substitutions had no effect (Fig. 2 *B*). An F246A substitution also reduced iC3b binding, although less dramatically than the F246K substitution (McGuire and Bajt, 1995). We have not included D248 and Y252 in our mutagenic approach since the respective side chains are not solvent-exposed (relative total side chain accessibility values were 0 and ~10%, respectively, in either conformation). Detrimental structural effects might have caused the defective binding of these mutants to iC3b.

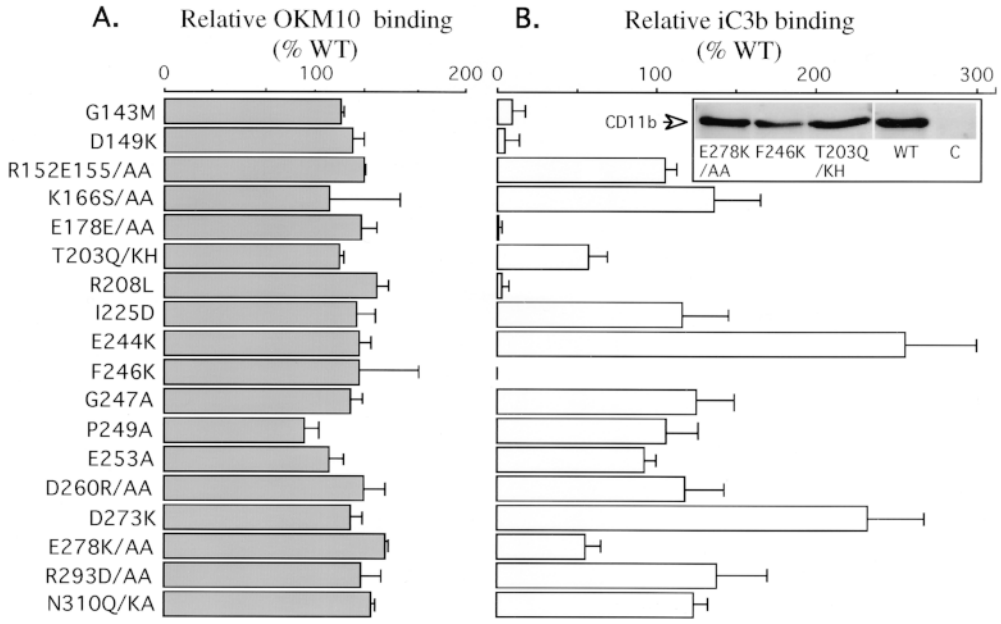

Figure 2. Effects of A-domain mutants on CR3 surface expression and iC3b binding. (*A*) Histograms (mean ± SEM, $n = 3$) showing the relative binding of anti-CD11b mAb OKM10 to COS cells expressing mutant CR3. (*B*) Histograms (mean ± SEM, $n = 3$) showing the relative binding of iC3b to COS cells expressing CR3 mutants. (*Inset*) Radioautograph of a Western blot showing comparable amounts of the CD11b subunit in anti-CD18 immunoprecipitates from COS cells expressing WT or mutant CR3. No CD11b was seen in anti-CD18 immunoprecipitates from COS cells transfected with CD18 cDNA alone.

Supportive evidence is provided by the finding that deletion of D248-Y252 led to the loss of CR3 binding to three different metal-dependent ligands including NIF (Zhang and Plow, 1996*b*). The present data reveal that residues from five different loops and two of their connecting helices contribute to the iC3b-binding site in r11bA.

The iC3b-binding Site Is Located on the MIDAS Face and Involves Conformationally Sensitive Residues

The residues involved in iC3b binding mapped to the MIDAS face of r11bA, in close proximity to the metal ion (Fig. 3). Two other ligands, NIF and CD54, also require residues expressed on the MIDAS face for interaction with CD11b and CD11a receptors, respectively (Rieu et al., 1994; Huang and Springer, 1995). The divalent cation–dependent interaction of iC3b with CR3 or its isolated r11bA requires key glutamate residues in iC3b (Taniguchi-Sidle and Isenman, 1994). The ring-like arrangement of the iC3b-binding site around the metal ion lends support to our hypothesis that the exogenous metal-coordinating glutamate in the open structure may be a mimic

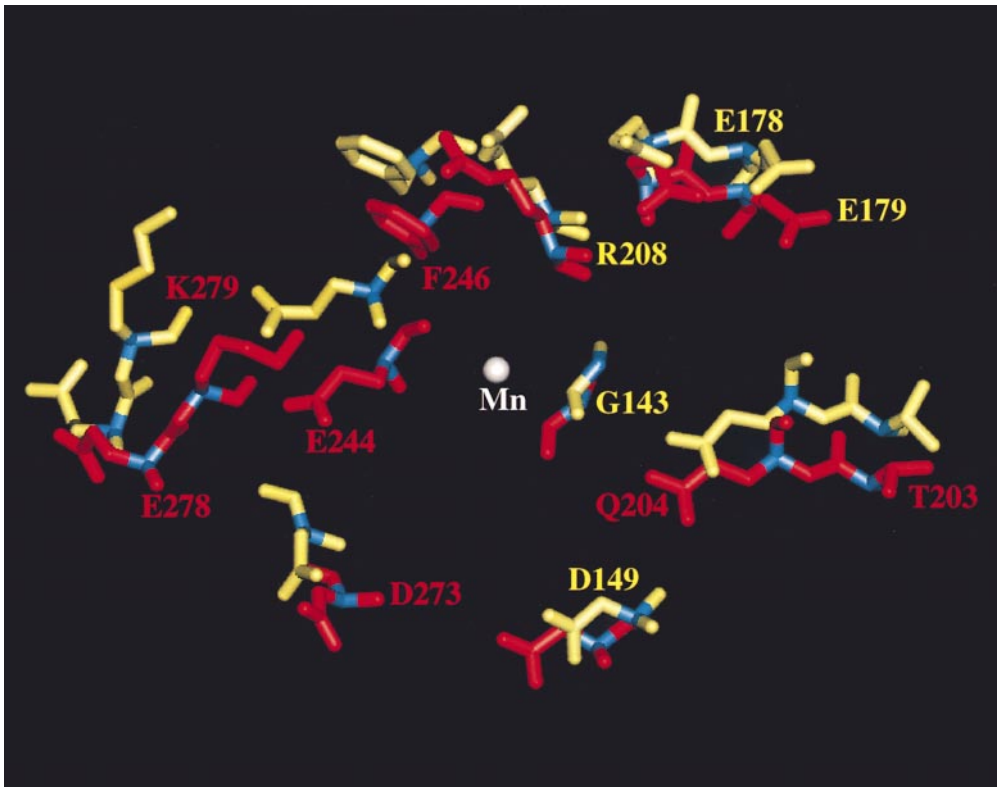

Figure 3. Protein movements of the iC3b-binding site in the two structures. Position of the side chains of residues involved in iC3b binding on MIDAS relative to Mn (*white ball*) in the open (*red*) and closed (*yellow*) structures. The residues that are also involved in NIF binding, G143, D149, E178E, and R208 (based on single or double amino acid substitutions) (Rieu et al., 1996), undergo little movement in the two structures (see also Table II).

Table II. Conformational Sensitivity of the Amino Acids Involved in iC3b Binding

Cα-metal distance (Å)*			Cα-metal distance (Å)		
aa	(Open/Closed)	Δ (Å)	aa	(Open/Closed)	Δ (Å)
T203	15.42/15.35	0.07	G143	5.70/6.20	0.50
Q204	11.66/11.70	0.04	D149	11.70/11.30	0.40
F246	6.50/9.00	2.50	E178	9.50/10.80	1.30
E244	5.50/7.30	1.80	E179	12.10/13.20	1.10
D273	11.30/10.10	1.20	R208	5.60/6.60	1.00
E278	16.00/18.30	2.30			
K279	13.30/16.80	3.50			

*Distances in angstroms are measured from the α carbon atom of each residue in the open and closed conformation to the respective metal ion. The residues that only affect iC3b binding are shown at the left, whereas those that also affect NIF binding are shown at the right.

of an integrin interaction with ligand (Lee et al., 1995*b*). Recent docking of collagen and CD54 ligands on the A-domains of CD49b and CD11a, respectively, showed that the respective glutamates can be accommodated in the A-domain without severe steric clashes, suggesting that the metal ion in the A-domain can coordinate the glutamate "ligands" directly (Emsley et al., 1997; Bella et al., 1998). Co-crystals of the A-domain in complex with activation-dependent and -independent ligands will be required to determine if the metal ion contributes directly to ligand coordination.

The residues G143, D149, R208, and E178E that are shared by the binding sites for iC3b and NIF (an activation-independent ligand) are located on one side of the metal ion (Fig. 3). Interestingly, the relative position of these residues in relation to the metal ion changed little (the Cα-metal ion distances generally ≤1 Å) in the open and closed conformations (Table II). In contrast, the relative position of most of the residues which selectively affect iC3b binding changed significantly in the two conformations with respect to the metal ion (Cα-metal ion distances changed by several angstroms in some cases) (Table II). Thus, a major distinguishing feature between the open and closed conformations, namely the change in topology on the MIDAS face, may be relevant to the activation-dependent binding of CR3 to iC3b. Conformational changes on the MIDAS face may be required to develop an optimal binding interface between CR3 and its physiologic ligands.

Effects of F302W or F275R Substitutions on Receptor Binding to iC3b, NIF, and mAb 7E3

A second structural difference between the open and closed r11bA conformations is a major increase in the solvent accessibility of the conserved F302 and F275 in the open conformation (relative total side chain accessibility values increase from 6.4 to 81.5% for F302 and from 0.3 and 26.4% for F275). Therefore, we assessed the effects of introducing bulky or charged side chains at these positions on the activation-dependent interaction of CR3 with iC3b. F302 was replaced with arginine, tryptophan, or tyrosine (as a control), and F275 was replaced with arginine. The CR3 mutant F302R was not expressed on the cell surface (data not shown). The remaining mutants were surface expressed in normal quantities relative to the WT receptor (Fig. 4 *A*). To determine the functional profile of the resulting mutants, the recombinant receptors were probed with the activation-dependent and -independent ligands iC3b and NIF, respectively. Whereas the binding of iC3b to the conserved F302Y receptor was indistinguishable from that of WT, iC3b binding to F302W and F275R was significantly increased (Fig. 4 *B*). On the other hand, NIF bound equally to F302Y, F302W, and F275R receptors. Similar observations were obtained in stable CHO cell lines expressing comparable amounts of WT or F302W (Fig. 4 *C*). Increased binding of F302W was not limited to iC3b, but also occurred with fibrinogen, another activation-dependent ligand (Fig. 4 *C*).

The 11bA recognizing mAb 7E3 (Zhou et al., 1994) is a ligand-mimetic antibody whose binding to the holoreceptor in leukocytes or in cells transfected with recombinant CR3 is stimulated by the same agonists that trigger physiologic ligand binding (Altieri and Edgington, 1988; Altieri, 1991; Simon et al., 1997). 7E3 is thus very useful in detecting high affinity CR3 in intact cells. The estimate of the later species is ~10% when 7E3 or a second ligand mimetic mAb CBRM1/5 (Diamond and Springer, 1993; Simon et al., 1997) is used. To assess the impact of the F302W modification on affinity modulation in CR3, we compared the binding of 7E3 to CHO cells expressing WT

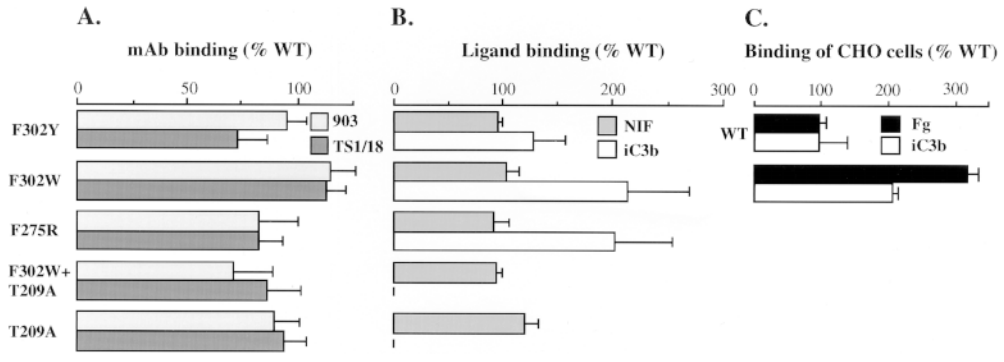

Figure 4. Effects of mutations involving F302, F275, and T209 on iC3b, fibrinogen, and NIF binding to recombinant membrane-bound CR3. (*A*) Histograms (mean ± SEM, $n = 3$) showing the normal cell surface expression of the mutant CR3 on transfected COS cells, as checked by anti-CD11b mAb 903 and anti-CD18 mAb TS1/18. (*B*) Histograms (mean ± SEM, $n = 4$) showing the binding of mutant CR3 expressed on COS cells to iC3b and NIF. (*C*) Histograms (mean ± SEM, $n = 3$) showing the binding of WT or F302W CR3-transfected CHO cells to iC3b and fibrinogen (*Fg*). The surface expression levels of both WT and F302W receptors were ~70% (data not shown).

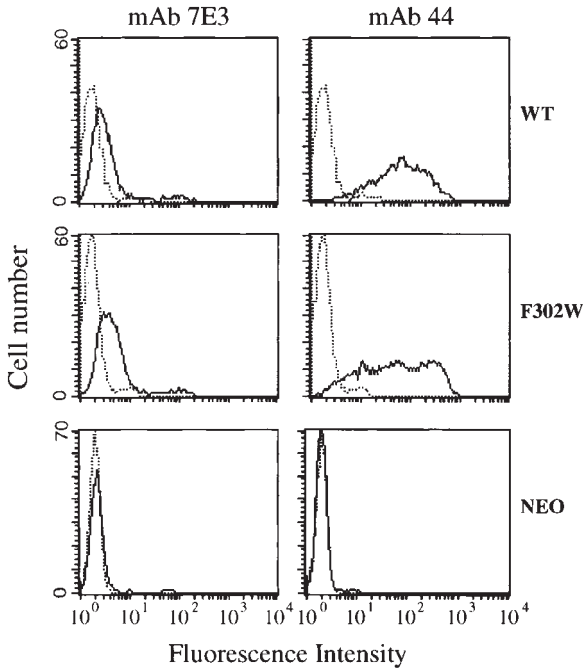

Figure 5. Interaction of mAb 7E3 with WT or F302W-transfected CHO cells. Expression of the activation-specific 7E3 epitope on WT, F302W, or Neo-transfected CHO cells was examined by flow cytometry. mAb 44, which recognizes the whole population of CR3, was used as a reference. Mouse IgG1 (*dotted lines*) was used to determine background fluorescence. The fraction of CR3 recognized by 7E3 is 5.95 ± 1.16% for WT and 14.9 ± 3.47% for F302W (n = 6).

or F302W CR3. In six independent experiments (one of which is shown in Fig. 5), we found that the fraction of CR3 recognized by 7E3 was 5.95 ± 1.6% of total CR3 for WT and 14.9 ± 3.47% for F302W. Thus the F302W substitution increases the fraction of high affinity CR3 in whole cells. Increased binding of iC3b and 7E3 to F302W r11bA was also observed (Fig. 6), whereas binding of NIF was unchanged. Taken together, the above findings indicate that a conformational change intrinsic to the A-domain enhances the binding of the holoreceptor as well as the isolated A-domain to activation-dependent ligands. Since 7E3 is a marker of the high affinity state, the observed increase in receptor binding appears to largely result from a change in receptor affinity.

Binding Properties of the T209A Receptor

The third major distinguishing feature between the two r11bA conformations is the shift in metal coordination from a direct coordination of T209 with the metal in the open form to a break in T209–metal bond in the closed form (Fig. 1). We assessed the functional significance of this shift on metal binding and receptor activation. We first reasoned that if the two Mn^{2+}-containing structures have biologic relevance, then a T209A mutation should not compromise the ability of r11bA to bind the metal ion. This was in fact the case: the normally expressed (Fig. 4 *A*) and heterodimeric (Kamata et al., 1995*b*; and data not shown) T209A CR3 bound normally to the activation-independent ligand NIF (Fig. 4 *B*). Since NIF binding requires divalent cations and an intact MIDAS (the metal-defective CR3 mutants D140GS/AGA or D242A do not bind to NIF [Rieu et al., 1994]), this finding indicates that the T209A CR3 can coordinate the metal ion in the MIDAS site. We then assessed the effect of T209A on receptor activation as quantified by binding to iC3b. As shown in Fig. 4 *B*, T209A receptor did not bind to iC3b in the presence of divalent cations. Similar results were obtained when binding of NIF and iC3b to the isolated T209A A-domain was carried out (Fig. 6). Interestingly, introducing the F302W mutation in T209A failed to restore any binding of the double mutant to iC3b (Fig. 4 *B*). A previous study (Kamata et al., 1995*b*) showed that a T209A mutation in the holoreceptor abolished its ability to bind to another activation-dependent ligand CD54, but suggested that this was caused by loss of metal coordination. The present findings clearly show an intact metal coordination site in the T209A mutant as judged by the normal binding of NIF. Therefore, these data suggest that direct coordination of the metal ion by T209 (as in the open conformation) is a necessary feature of the activated state. Switching this coordination from T209 to D242 as in the closed

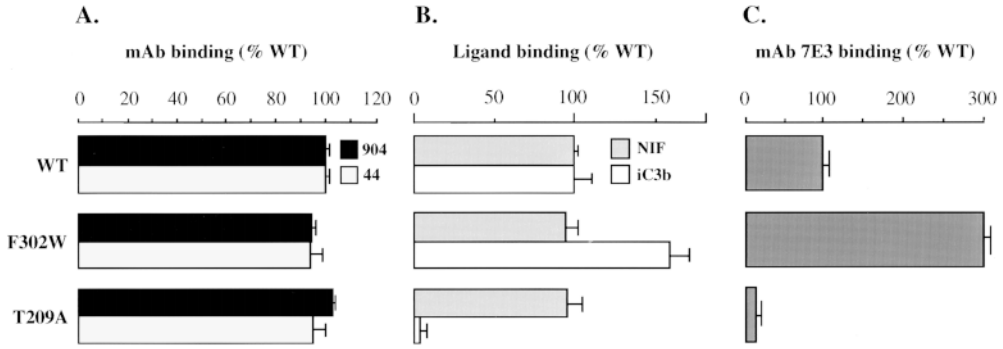

Figure 6. Effects of F302W and T209A on direct binding of purified r11bA to iC3b, NIF, and mAb 7E3. (*A*) Histograms (mean ± SEM, n = 3) showing that equivalent amounts of WT and mutant r11bA were immobilized onto 96-well plates. (*B*) Histograms (mean ± SEM, n = 5) showing a selective gain of binding of F302W to iC3b but not to NIF, and a selective loss of binding of T209A to iC3b but not to NIF. (*C*) Histograms (mean ± SEM, n = 4) showing a gain of F302W binding to mAb 7E3 and a loss of T209A binding to this mAb.

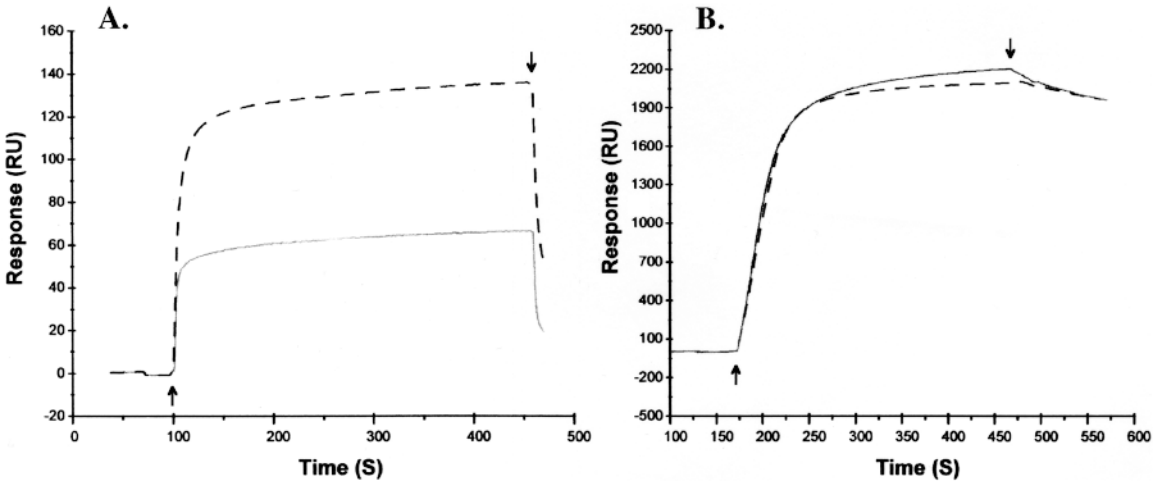

Figure 7. Sensorgrams recording interactions of WT or F302W A-domains with immobilized iC3b and mAb 904. Overlay plot of sensorgrams recorded the injection of 1 μM of WT (*solid lines*) or F302W (*dashed lines*) A-domains at a flow rate of 5 μl/min for 6 min through the iC3b- (*A*) or mAb 904–coated (*B*) chips. Arrows indicate the beginning and end of injection.

conformer generates an inactive receptor. Taken together, the above data show that all three features of the open conformation (the change in the topology of the MIDAS face, the solvent accessibility of side chains at positions 302 and 275, and the direct coordination of the metal by T209) are relevant to enhancing CR3 or r11bA binding to activation-dependent ligands, suggesting a functional significance for these linked structural features.

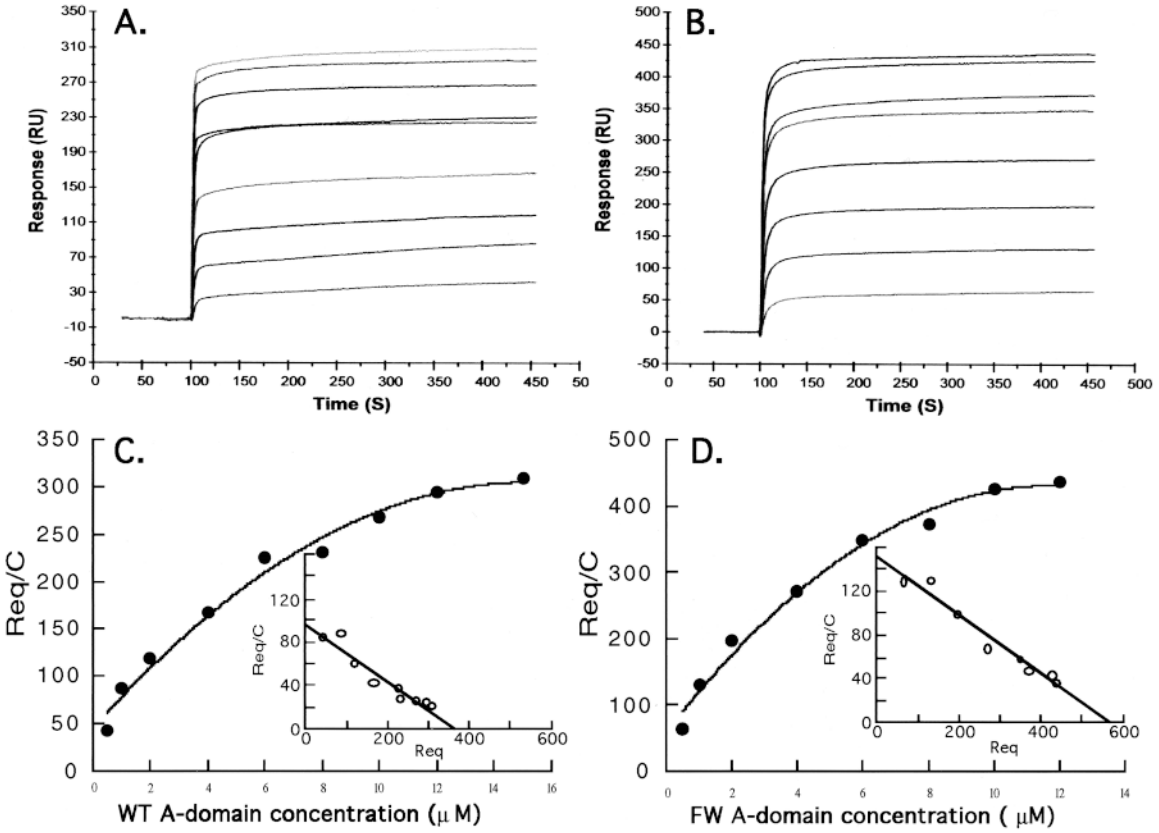

Figure 8. Equilibrium analysis of the interaction of WT or F302W A-domains with immobilized iC3b. Concentrations ranging from 0.5 to15 μM for WT (*A*) and 0.5 to 12 μM for F302W (*B*) were injected at a flow rate of 5 μl/min for 6 min to reach equilibrium. *C* (for WT) and *D* (for F302W) show the respective saturable binding curves and Scatchard plots (*insets*).

Two Functional States for the A-Domain Exist in Solution: Effect of the F302W Mutation on the Active State

A simple model that explains the above functional and structural studies is that the isolated r11bA exists in two functional states in solution, one active (defined by its ability to bind to activation-dependent ligands) and the other inactive (although still able to bind certain antagonists such as NIF). Activating mutations (such as F302W) or inactivating mutations (such as T209A) change the relative abundance of these two states. To test this model, we used surface plasmon resonance (Malmqvist, 1993) and examined the binding of WT and F302W r11bA to iC3b and mAb 904, an activation-independent and metal-independent ligand. When 1 μM of WT and F302W was injected onto the BIAcore™ sensor chip coupled to excess iC3b, an approximately twofold increase in binding of F302W was observed compared with WT (Fig. 7 *A*), in agreement with the other binding data presented in Figs. 4–6. When the same amounts of WT and F302W were injected onto the mAb 904–coupled chip surface, no difference in the binding level was found (Fig. 7 *B*). This indicates that equivalent amounts of WT and F302W r11bA were available for binding. Injection of increasing concentrations of the WT r11bA ranging from 0.5 to 15 μM at a flow rate of 5 μl/min gave a saturable binding curve (Fig. 8, *A* and *C*). Scatchard plot of the binding data was linear, with a dissociation constant K_d of 3.8 μM (Fig. 8 *C*). A similar analysis using F302W revealed an almost identical affinity (Fig. 8, *B* and *D*). The observed ligand-binding affinity was significantly lower than that reported for binding of purified CR3 to ligands (K_d ~12.5–200 nM) (Berman et al., 1993; Cai and Wright, 1995). One interpretation for this difference is that the A-domain preparation contains only a subpopulation of active species. Biosensor technology can be used to measure the active analyte in a protein preparation under conditions where binding to ligand (present in excess) is only limited by the diffusion of the analyte to the surface-bound ligand. Under these conditions, initial binding rates are proportional to the active analyte concentration and independent of the analyte-ligand affinity. This can be validated experimentally by demonstrating that the initial binding rate is independent of ligand density (Karlsson et al., 1993). We used mAb 904 in parallel in order to estimate total binding. By decreasing the flow rate and increasing the ligand density, the binding rate of WT and F302W r11bA to chips coated with iC3b or mAb 904 can be made independent of the respective ligand density (Table III) and therefore a function of the concentration of the binding active species. In WT, this active species represented ~11 ± 1.7% of the total r11bA (Table IV). In parallel experiments, we showed that the proportion of the active species in F302W increased by ~2.5-fold (25 ± 1.1%). The fact that a major portion of F302W remains in the inactive state probably reflects other structural considerations that allow motion of the α7 helix to that of the closed form, despite a partial burial of the side chain at position 302. The recent structure of the CD49b A-domain shows that this does in fact occur: the orientation of the α7 helix is very similar to that in the closed form of r11bA, despite only a partial burial of the side chain of E318 (equivalent to F302) at the top of the α7 helix (Emsley et al., 1997). Since, the total amount of r11bA was used in calculating the binding affinities shown in Fig. 8, the affinity of the active species should be ~10-fold higher, approaching that calculated for purified CR3 and of the active cell-bound form of CD11a/CD18 (Lollo et al., 1993).

In summary, the r11bA exists in two functional states in solution as assessed by BIAcore™. These two forms are equally capable of interacting with activation-independent ligands such as NIF, but display marked differences in their affinity to physiologic ligands such as iC3b, fibrinogen, and the ligand mimetic mAb 7E3. The two states appear to be in a dynamic equilibrium with a majority of the domain in an inactive state (defined as one incapable of binding to activation-dependent ligands, due to the lack of an activation-specific ligand-binding interface). This equilibrium can be modulated both positively or negatively by certain mutations (described in this report) and perhaps by others (Zhang and Plow, 1996*a*). Based on the functional analysis of the various A-domain mutants, we also suggest that the active and inactive states may correspond to the open and closed structures, respectively. In this scenario, analogous movement of the COOH-terminal α7 helix of the A-domain in the holoreceptor switches the receptor to its active state. Since a MIDAS-like ligand-binding motif is present in all β subunits, an affinity switch not unlike that of G proteins may be operational on the extracellular face in all integrins.

Table III. Initial Binding Rates of WT and F302W on iC3b and mAb 904 Surfaces with Two Different Ligand Densities

		Initial binding rates (RU/S)			
		iC3b*		mAb 904	
	nM	6,300 RU	8,000 RU	4,200 RU	6,200 RU
WT	200	1.96	1.93	16.5	18.3
	500	5.32	5.83	41.7	39.9
F302W	200	4.14	4.38	15.9	17.1
	500	11.8	12.2	40.1	43.1

*No significant differences in binding rates were observed from two different surfaces of iC3b and 904, indicating the rates were independent of ligand density, therefore they were mass transfer limiting binding rates.

Table IV. Initial Binding Rates of WT and F302W on iC3b and mAb 904 Surfaces with High Ligand Densities (>8,000 RU for iC3b, >6,000 RU for mAb 904), and Relative Percentages of Active Proportions of A-Domain Proteins

	Initial binding rates (RU/S)					
	iC3b		mAb 904		% active	
nM	WT	F302W	WT	F302W	WT	F302W
37.5	0.68	1.33	5.84	5.64	11.6	23.6
75	1.48	2.81	12.0	11.2	12.3	25.1
150	2.15	5.71	23.7	22.1	9.1	25.8

Data shown are from one representative experiment out of three performed.

We thank Drs. Shu-Ichi Kanazachi for protein purification; George Chen and Takashi Sugimori for plasmid constructs; Alain Viel, Ben Madden, Andrew Tyler, and Ashok Khatri for assistance in protein characterization; and Lonny Berman and his staff at beamline X25 of the Brookhaven National Light Source for assistance in data collection.

Grants from the National Institutes of Health and a fellowship grant from the American Heart Association and the Philippe Foundation supported this work. The Brookhaven National Light Source Facility is supported by the US Department of Energy, Office of Health and Environmental Research, and by the National Science Foundation.

Received for publication 14 May 1998 and in revised form 4 September 1998.

References

Altieri, D.C. 1991. Occupancy of CD11b/CD18 (Mac-1) divalent ion binding site(s) induces leukocyte adhesion. *J. Immunol.* 147:1891–1896.

Altieri, D.C., and T.S. Edgington. 1988. The saturable high affinity association of factor X to ADP-stimulated monocytes defines a novel function of the MAC-1 receptor. *J. Biol. Chem.* 263:7007–7015.

Andrew, D.P., C. Berlin, S. Honda, T. Yoshino, A. Hamann, B. Holzmann, P.J. Kilshaw, and E.C. Butcher. 1994. Distinct but overlapping epitopes are involved in alpha 4 beta 7-mediated adhesion to vascular cell adhesion molecule-1, mucosal addressin-1, fibronectin, and lymphocyte aggregation. *J. Immunol.* 153:3847–3861.

Arnaout, M.A., R.F. Todd III, N. Dana, J. Melamed, S.F. Schlossman, and H.R. Colten. 1983. Inhibition of phagocytosis of complement C3- or immunoglobulin G–coated particles and of iC3b binding by monoclonal antibodies to a monocyte-granulocyte membrane glycoprotein (Mo1). *J. Clin. Invest.* 72: 171–179.

Bajt, M.L., and J.C. Loftus. 1994. Mutation of a ligand binding domain of β3 integrin: integral role of oxygenated residues in $\alpha_{IIb}\beta_3$ (GPIIb-IIIa) receptor function. *J. Biol. Chem.* 269:20913–20919.

Baldwin, E.T., R.W. Sarver, G.L. Bryant, K.A. Curry, M.B. Fairbanks, B.C. Finzel, R.L. Garlick, R.L. Heinrikson, N.C. Horton, L.-L.C. Kelley, et al. 1998. Cation binding to CD11b I domain and activation model assessment. *Structure.* 6:923–935.

Bella, J., P.R. Kolatkar, C.W. Marlor, J.M. Greve, and M.G. Rossmann. 1998. The structure of the two amino-terminal domains of human ICAM-1 suggests how it functions as a rhinovirus receptor and as an LFA-1 integrin ligand. *Proc. Natl. Acad. Sci. USA.* 95:4140–4145.

Berman, P.W., G. Nakamura, L. Riddle, H. Chiu, K. Fisher, M. Champe, A. Gray, and S. Fong. 1993. Biosynthesis and function of membrane bound and secreted forms of recombinant Mac-1. *J. Cell Biochem.* 52:183–195.

Bilsland, C.A.G., M.S. Diamond, and T.A. Springer. 1994. The leukocyte integrin p150,95 (Cd11c/CD18) as a receptor for iC3b. *J. Immunol.* 152:4582–4589.

Cai, T.Q., and S.D. Wright. 1995. Energetics of leukocyte integrin activation. *J. Biol. Chem.* 270:14358–14365.

Clackson, T., and J.A. Wells. 1995. A hot spot of binding energy in a hormone-receptor interface. *Science.* 267:383–386.

Coller, B.S. 1985. A new murine monoclonal antibody reports an activation-dependent change in the conformation and/or microenvironment of the platelet glycoprotein IIb/IIIa complex. *J. Clin. Invest.* 76:101.

D'Souza, S.E., M.H. Ginsberg, T.A. Burke, S.C.-T. Lam, and E.F. Plow. 1988. Localization of an Arg-Gly-Asp recognition site within an integrin adhesion receptor. *Science.* 242:91–93.

D'Souza, S.E., T.A. Haas, R.S. Piotrowicz, W.V. Byers, D.E. McGrath, H.R. Soule, C. Cierniewski, E.F. Plow, and J.W. Smith. 1994. Ligand and cation binding are dual functions of a discrete segment of the integrin beta 3 subunit: cation displacement is involved in ligand binding. *Cell.* 79:659–667.

Dall'Acqua, W., E.R. Goldman, E. Eisenstein, and R.A. Mariuzza. 1996. A mutational analysis of the binding of two different proteins to the same antibody. *Biochemistry.* 35:9667–9676.

Dana, N., B. Styrt, G.D. Griffin, R.F. Todd III, M.S. Klempner, and M.A. Arnaout. 1986. Two functional domains in the phagocyte membrane glycoprotein Mo1 identified with monoclonal antibodies. *J. Immunol.* 137:3259–3263.

Deng, W.P., and J.A. Nicoloff. 1992. Site-directed mutagenesis of virtually any plasmid by eliminating a unique site. *Anal. Biochem.* 200:81–88.

Diamond, M.S., and T.A. Springer. 1993. A subpopulation of Mac-1 (CD11b/CD18) molecules mediates neutrophil adhesion to ICAM-1 and fibrinogen. *J. Cell Biol.* 120:545–556.

Diamond, M.S., J. Garcia-Aguilar, J.K. Bickford, A.L. Corbi, and T.A. Springer. 1993. The I domain is a major recognition site on the leukocyte integrin Mac-1 (CD11b/CD18) for four distinct adhesion ligands. *J. Cell Biol.* 120:1031–1043.

Dransfield, I., C. Cabanas, J. Barrett, and N. Hogg. 1992. Interaction of leukocyte integrins with ligand is necessary but not sufficient for function. *J. Cell Biol.* 116:1527–1535.

Du, X., M. Gu, J.W. Weiel, C. Nagaswami, J. Bennet, R. Bowdicth, and M.H. Ginsberg. 1993. Long range propagation of conformational changes in integrin aIIbb3. *J. Biol. Chem.* 268:23087–23092.

Emsley, J., S.L. King, J.M. Bergelson, and R.C. Liddington. 1997. Crystal structure of the I domain from integrin alpha2beta1. *J. Biol. Chem.* 272:28512–28517.

Finzel, B.C. 1987. Incorporation of fast Fourier transforms to speed restrained least-squares refinement of protein structures. *J. Appl. Crystalog.* 20:53–55.

Golenbock, D.T., Y. Liu, F.H. Millham, M.W. Freeman, and R.A. Zoeller. 1993. Surface expression of human CD14 in Chinese hamster ovary fibroblasts imparts macrophage-like responsiveness to bacterial endotoxin. *J. Biol. Chem.* 268:22055–22059.

Huang, C., and T.A. Springer. 1995. A binding interface on the I domain of lymphocyte function-associated antigen-1 (LFA-1) required for specific interaction with intercellular adhesion molecule 1 (ICAM-1). *J. Biol. Chem.* 270:19008–19016.

Hynes, R.O. 1992. Integrins: versatility, modulation and signaling in cell adhesion. *Cell.* 69:11–26.

Kamata, T., and Y. Takada. 1994. Direct binding of collagen to the I domain of integrin $\alpha_2\beta_1$ (VLA-2, CD49b/CD29) in a divalent cation-independent manner. *J. Biol. Chem.* 269:26006–26010.

Kamata, T., W. Puzon, and Y. Takada. 1995*a*. Identification of putative ligand-binding sites of the integrin α4β1. *Biochem. J.* 305:945–951.

Kamata, T., R. Wright, and Y. Takada. 1995*b*. Critical threonine and aspartic acid residues within the I domains of beta 2 integrins for interactions with intercellular adhesion molecule 1 (ICAM-1) and C3bi. *J. Biol. Chem.* 2705: 12531–12535.

Karlsson, R., L. Fagerstam, H. Nilshans, and B. Persson. 1993. Analysis of active antibody concentration. Separation of affinity and concentration parameters. *J. Immunol. Methods.* 166:75–84.

Kunkel, T.A., J.D. Roberts, and R.A. Zakour. 1987. Rapid and efficient site-specific mutagenesis without phenotypic selection. *Methods Enzymol.* 154: 367–382.

Laemmli, U.K. 1970. Cleavage of structural proteins during the assembly of the head of bacteriophage T_4. *Nature.* 227:680–685.

Landis, R.C., R.I. Bennett, and N. Hogg. 1993. A novel LFA-1 activation epitope maps to the I domain. *J. Cell Biol.* 120:1519–1527.

Landis, R.C., A. McDowall, C.L. Holness, A.J. Littler, D.L. Simmons, and N. Hogg. 1994. Involvement of the "I" domain of LFA-1 in selective binding to ligands ICAM-1 and ICAM-3. *J. Cell Biol.* 126:529–537.

Lee, J.-O., L. Anne-Bankston, M.A. Arnaout, and R.C. Liddington. 1995*a*. Two conformations of the integrin A-domain (I-domain): a pathway for activation? *Structure.* 3:1333–1340.

Lee, J.-O., P. Rieu, M.A. Arnaout, and R. Liddington. 1995*b*. Crystal structure of the A-domain from the α-subunit of β2 integrin complement receptor type 3 (CR3, CD11b/CD18). *Cell.* 80:631–638.

Lollo, B.A., K.W.H. Chan, E.M. Hanson, V.T. Moy, and A.A. Brian. 1993. Direct evidence for two affinity states for lymphocyte function-associated antigen 1 on activated T cells. *J. Biol. Chem.* 268:21693–21700.

Malmqvist, M. 1993. Biospecific interaction analysis using biosensor technology. *Nature.* 361:186–187.

Maniatis, T., E.F. Fritch, and J. Sambrook. 1989. Molecular Cloning: A Laboratory Manual. 2nd edition. Cold Spring Harbor Laboratory, Cold Spring Harbor, New York.

McGuire, S.L., and M.L. Bajt. 1995. Distinct ligand binding sites in the I domain of integrin alpha M beta 2 that differentially affect a divalent cation-dependent conformation. *J. Biol. Chem.* 270:25866–25871.

Michishita, M., V. Videm, and M.A. Arnaout. 1993. A novel divalent cation-binding site in the A domain of the β2 integrin CR3 (CD11b/CD18) is essential for ligand binding. *Cell.* 72:857–867.

Otwinowski, Z. 1991. Maximum likelihood refinement of heavy atom parameters. *In* Isomorphous Replacement and Anomalous Scattering. W. Wolf, P.R. Evans, and A.G.W. Leslie, editors. Science and Engineering Research Council, Darensbury Laboratory. 80–86.

Pytela, R. 1988. Amino acid sequence of murine Mac-lα chain reveals homology with the integrin family and an additional domain related to von Willebrand factor (VWF). *EMBO (Eur. Mol. Biol. Organ.) J.* 7:1371–1378.

Qu, A., and D.J. Leahy. 1995. Crystal structure of the I-domain from the CD11a/CD18 (LFA-1, αLβ2) integrin. *Proc. Natl. Acad. Sci. USA.* 92:10277–10281.

Qu, A., and D.J. Leahy. 1996. The role of the divalent cation in the structure of the I domain from the CD11a/CD18 integrin. *Structure.* 4:931–942.

Randi, A.M., and N. Hogg. 1994. I domain of β2 integrin lymphocyte-associated-antigen 1 contains a binding site for ligand intercellular adhesion molecule-1. *J. Biol. Chem.* 269:12395–12398.

Rieu, P., T. Sugimori, D.L. Griffith, and M.A. Arnaout. 1996. Solvent accessible residues on the MIDAS face of integrin CR3 mediate its binding to the neutrophil adhesion inhibitor NIF. *J. Biol. Chem.* 271:15858–15861.

Rieu, P., T. Ueda, I. Haruta, C.P. Sharma, and M.A. Arnaout. 1994. The A-domain of β2 integrin CR3 (CD11b/CD18) is a receptor for the hookworm-derived neutrophil adhesion inhibitor NIF. *J. Cell Biol.* 127:2081–2091.

Ross, G.D., J.A. Cain, B.L. Myones, S.L. Newman, and P.J. Lachmann. 1987. Specificity of membrane complement receptor type three (CR3) for beta-glucans. *Complement.* 4:61–74.

Sanger, F., S. Nicklen, and A.R. Coulson. 1977. DNA sequencing with chain terminating inhibitors. *Proc. Natl. Acad. Sci. USA.* 74:5463–5467.

Simon, D.I., H. Xu, S. Ortlepp, C. Rogers, and N.K. Rao. 1997. 7E3 monoclonal antibody directed against platelet glycoprotein IIb/IIIa cross-reacts with the leukocyte integrin Mac-1 and blocks adhesion to fibrinogen and ICAM-1. *Arterioscler. Thromb. Vasc. Biol.* 17:528–535.

Smith, J.W., and D.A. Cheresh. 1988. The Arg-Gly-Asp binding domain of the vitronectin receptor. *J. Biol. Chem.* 263:18726–18731.

Taniguchi-Sidle, A., and D.E. Isenman. 1994. Interactions of human complement component C3 with factor B and with complement receptors type 1 (CR1, CD35) and type 3 (CR3, CD11b/CD18) involve an acidic sequence at the N-terminus of C3 alpha-chain. *J. Immunol.* 153:5285–5302.

Tuckwell, D., D.A. Calderwood, L.J. Green, and M.J. Humphries. 1995. Integrin α2 I-domain is a binding site for collagens. *J. Cell Sci.* 108:1629–1637.

Ueda, T., P. Rieu, J. Brayer, and M.A. Arnaout. 1994. Identification of the complement iC3b binding site in the β2 integrin CR3 (CD11b/CD18). *Proc. Natl. Acad. Sci. USA.* 91:10680–10684.

Wright, S.D., P.A. Reddy, M.T.C. Jong, and B.W. Erickson. 1987. C3bi receptor (complement receptor type 3) recognizes a region of complement protein C3 containing the sequence arg-gly-asp. *Proc. Natl. Acad. Sci. USA.* 84:1965–1968.

Xie, J., R. Li, P. Kotovuori, C. Vermot-Desroches, J. Wijdenes, M.A. Arnaout, P. Nortamo, and C.G. Gahmberg. 1995. Intercellular adhesion molecule-2 (CD102) binds to the leukocyte integrin CD11b/CD18 through the A domain. *J. Immunol.* 155:3619–3628.

Zhang, L., and E.F. Plow. 1996*a*. A discrete site modulates activation of I domains. *J. Biol. Chem.* 271:29953–29957.

Zhang, L., and E.F. Plow. 1996*b*. Overlapping, but not identical sites are involved in the recognition of C3bi, neutrophil inhibitory factor, and adhesive ligands by the αMβ2 integrin. *J. Biol. Chem.* 271:18211–18216.

Zhou, L., D.H. Lee, J. Plescia, C.Y. Lau, and D.C. Altieri. 1994. Differential ligand binding specificities of recombinant CD11b/CD18 integrin I-domain. *J. Biol. Chem.* 269:17075–17079.